Fourteenth International Conference on Domain Decomposition Methods
Editors: Ismael Herrera , David E. Keyes, Olof B. Widlund, Robert Yates

15. Numerical Simulation of The Motion of Pendula in an Incompressible Viscous Fluid by Lagrange Multiplier/Fictitious Domain Methods

L. H. Juárez[1], R. Glowinski[2]

1. Introduction. Lagrange Multiplier/Fictitious Domain Methods have proved to be effective in the direct numerical simulation of the motion of rigid bodies in incompressible viscous fluids [7]. In this work we discuss the application of this methodology, combined with finite element approximations and operator splitting, to the numerical simulation of the motion of pendula in a Newtonian incompressible viscous fluid. The pendula are circular cylinders constrained to move in a circular trajectory. The motion of the cylinders are driven only by the hydrodynamical forces and gravity.

In the present calculations we allowed solid surfaces to touch and penetrate, contrary to what was done in previous work where these methods were applied [7]. In fact, a good feature of this methodology is that the numerical solution does not break down when the rigid bodies overlap. On the other hand, numerical methods in which the computational domain is remeshed may break down when collision occurs, because this would break the lattice modeling of the fluid [8]. Hence a repulsive force between the particles need to be incorporated when they are close to each other to prevent contact between surfaces. In the numerical simulations in this work we did not introduce these artificial repulsive forces, in part because we wanted to investigate the solutions when the rigid bodies are near collision or when they actually collide and overlap. The mechanics of how solid particles in viscous liquids stick or rebound has not been fully understood and is still subject of current research. It has been demonstrated theoretically that when a perfect rigid sphere approaches a rigid wall its kinetic energy is dissipated by non-conservative viscous forces. The rate of close approach is asymptotically slow and the sphere do not deform or rebound [2]. By simultaneously accounting for elastic deformation of the body and viscous fluid forces, Davis *et al.* [3] showed that part of the incoming particle kinetic energy is dissipated by fluid forces and internal solid friction, and the rest is transformed into elastic-strain energy of deformation. Depending on the fraction of the kinetic energy that becomes stored as elastic-strain energy, the deformation of the spheres may be significant and rebound may occur. The relevant parameter for the bouncing transition, which is often obtained experimentally [9], is the *Stokes number*, which characterize the particle inertia relative to viscous forces. Numerical results of colliding bodies in viscous fluids may help to understand the mechanics of individual collisions in solid-liquid flows, which is an important issue in particulate multi-phase flow modeling and in the actual numerical computations of these flows. The numerical experiments in this work include the motion of a single pendulum, and the motion of two pendula. The two pendula case include different numerical experiments where the disks may have different densities and initial positions. An interesting study of pendula in viscous fluids with some applications can be found in [12] and references therein.

In Section 2 we describe the model for a single pendulum. A Lagrange Multiplier/Fictitious Domain equivalent formulation is presented in Section 3. The discretization of the resulting problem is discused in Sections 4 and 5. Numerical results and conclusions are given in Section 6.

2. Fluid-Rigid Body Interaction Model. We describe the model for the case of one pendulum in a viscous fluid. Its generalization to several pendula is straightforward. Let $\Omega \subset \mathbb{R}^2$ be a space region with boundary Γ, filled with an *incompressible viscous fluid*,

[1]University of Houston and UAM-I, hector@math.uh.edu, and hect@xanum.uam.mx
[2]University of Houston, roland@math.uh.edu

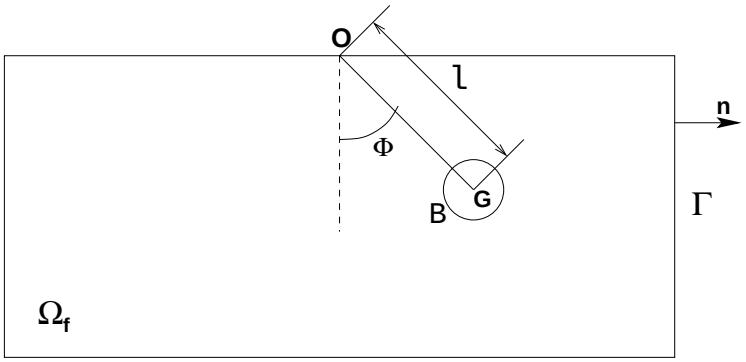

Figure 2.1: Pendulum in a viscous fluid

of density ρ_f, and that contains a rigid body B, with center of mass $\mathbf{G}$. The rigid body is constrained to move in a circular trajectory around the axis of rotation defined by a point $\mathbf{O}$, as shown in Figure 2.1. The position of the rigid body is known at any time t through the angle $\Phi = \Phi(t)$. We denote by $\mathbf{n}$ the unit normal vector pointing outward to the flow region $\Omega_f(t) = \Omega \setminus \overline{B}(t)$. Assuming that the only external force acting on the mixture is *gravity* (denoted by $\mathbf{g}$), in the vertical negative direction, the fluid flow is modeled by the *Navier-Stokes equations*

$$\rho_f \left[\frac{\partial \mathbf{u}}{\partial t} + (\mathbf{u} \cdot \boldsymbol{\nabla})\mathbf{u} \right] = \rho_f \mathbf{g} + \boldsymbol{\nabla} \cdot \boldsymbol{\sigma} \ in \ \Omega_f(t), \tag{2.1}$$

$$\boldsymbol{\nabla} \cdot \mathbf{u} = 0 \ in \ \Omega_f(t), \tag{2.2}$$

where $\mathbf{u}$ denotes the velocity of the fluid, p is the fluid pressure, and $\boldsymbol{\sigma} = \boldsymbol{\tau} - p\mathbf{I}$ is the *stress-tensor*, with $\boldsymbol{\tau} = \mu_f(\boldsymbol{\nabla}\mathbf{u} + \boldsymbol{\nabla}\mathbf{u}^t)$ for a *Newtonian fluid* with viscosity μ_f. These equations are completed by some *initial conditions* and by the following *no-slip boundary conditions*: $\mathbf{u} = \mathbf{0}$ *on* Γ, and $\mathbf{u}(\mathbf{x}, t) = \mathbf{V}(t) + \boldsymbol{\omega}(t) \times \overrightarrow{\mathbf{G}(t)\mathbf{x}}$, $\forall \mathbf{x} \in \partial B(t)$. Here $\mathbf{V}(t)$ and $\boldsymbol{\omega}(t)$ are the translational and angular velocities of the rigid body, respectively. The motion of the rigid body B is modeled by the *Newton-Euler* equations:

$$M\frac{d\mathbf{V}}{dt} = M\mathbf{g} + \mathbf{F}, \tag{2.3}$$

$$\mathbf{I}\frac{d\boldsymbol{\omega}}{dt} = \mathbf{T}, \tag{2.4}$$

where M and $\mathbf{I}$ are the *mass* and *inertia tensor* of the rigid body, respectively. $\mathbf{F}$ is the resultant of the *hydrodynamical forces* acting on B, and $\mathbf{T}$ is the *torque* at $\mathbf{G}$ of the above hydrodynamical forces acting on B. The previous equations are completed by the kinematic equations $d\mathbf{G}/dt = \mathbf{V}$, $d\boldsymbol{\Phi}/dt = \boldsymbol{\omega}$, and by imposing initial conditions on $\mathbf{G}$, $\boldsymbol{\Phi}$, $\mathbf{V}$, and $\boldsymbol{\omega}$. Here we use the notation $\boldsymbol{\omega} = (0, 0, \omega)$, and $\boldsymbol{\Phi} = (0, 0, \phi)$. Finally, the above equations are simplified by using the constraint relation $\mathbf{V} = \boldsymbol{\omega} \times \overrightarrow{\mathbf{GO}} = l\,\omega\,(cos\phi,\ sin\phi)$.

3. Fictitious Domain Formulation with Distributed Lagrange Multipliers. To obtain this formulation we fill the rigid bodies with the surrounding fluid, and compensate the above step by introducing an "antiparticle" of mass $-M\rho_f/\rho_B$ and inertia $-I\rho_f/\rho_B$. Finally we impose the rigid body motion on $\overline{B}(t)$ via a Lagrange multiplier $\boldsymbol{\lambda}$ supported by $\overline{B}(t)$. We obtain, then, a flow problem over the entire region Ω, for which the

global variational formulation is: *For $t > 0$, find* $\mathbf{u}(t) \in (H_0^1(\Omega))^2$, $p(t) \in L^2(\Omega)$, $\omega(t) \in R$, $\phi(t) \in R$, $\boldsymbol{\lambda}(t) \in \Lambda(t) = (H^1(B(t)))^2$ *such that*

$$\begin{cases} \rho_f \int_\Omega \left[\frac{\partial \mathbf{u}}{\partial t} + (\mathbf{u}\cdot\boldsymbol{\nabla})\mathbf{u}\right]\cdot \mathbf{v} d\mathbf{x} - \int_\Omega p\boldsymbol{\nabla}\cdot\mathbf{v} d\mathbf{x} + \mu_f \int_\Omega \boldsymbol{\nabla}\mathbf{u} : \boldsymbol{\nabla}\mathbf{v} d\mathbf{x} + \\ (1-\frac{\rho_f}{\rho_B})(Ml^2+I)\frac{d\omega}{dt}\theta - \langle \boldsymbol{\lambda}, \mathbf{v} - \boldsymbol{\theta}\times\overrightarrow{\mathbf{Ox}}\rangle_{\Lambda(t)} = \\ \rho_f \int_\Omega \mathbf{g}\cdot\mathbf{v}\, d\mathbf{x} - (1-\frac{\rho_f}{\rho_B})M\mathbf{g}\, l\, sin\phi\, \theta,\ \forall \mathbf{v} \in (H_0^1(\Omega))^2,\ \ \forall \theta \in R, \end{cases} \tag{3.1}$$

$$\int_\Omega q\boldsymbol{\nabla}\cdot\mathbf{u}(t) d\mathbf{x} = 0,\ \forall q \in L^2(\Omega), \tag{3.2}$$

$$\langle \boldsymbol{\mu}, \mathbf{u}(t) - \boldsymbol{\omega}(t)\times\overrightarrow{\mathbf{Ox}}\rangle_{\Lambda(t)} = 0,\ \forall \boldsymbol{\mu} \in \Lambda(t), \tag{3.3}$$

$$\frac{d\phi}{dt} = \omega, \tag{3.4}$$

$$\omega(0) = \omega^0,\ \phi(0) = \phi^0, \tag{3.5}$$

$$\mathbf{u}(\mathbf{x}, 0) = \mathbf{u}_0(\mathbf{x})\ in\ \Omega,\ with\ \mathbf{u}_0(\mathbf{x}) = \boldsymbol{\omega}^0 \times \overrightarrow{\mathbf{Ox}}\ in \overline{B(0)}, \tag{3.6}$$

A natural choice for $< \cdot, \cdot >$ is defined by

$$< \boldsymbol{\mu}, \mathbf{v} >= \int_{B(t)} (\boldsymbol{\mu}\cdot\mathbf{v} + \delta^2 \boldsymbol{\nabla}\boldsymbol{\mu} : \boldsymbol{\nabla}\mathbf{v}) d\mathbf{x},\ \forall \boldsymbol{\mu},\ \mathbf{v} \in \Lambda(t), \tag{3.7}$$

with δ a *characteristic length* (the diameter of B, for example).

4. The Finite Element Discretization. We assume that Ω is a polygonal domain in R^2. Let $h(= h_\Omega)$ be a *space discretization step*, $\mathcal{T}_h$ a finite element triangulation of $\overline{\Omega}$, and P_s the space of polynomials in two variables of degree $\leq s$. The functional spaces $(H^1(\Omega))^2$ for velocity, and $L^2(\Omega)$ for pressure, are approximated by the following finite dimensional spaces

$$V_h = \{\mathbf{v}_h \in (C^0(\overline{\Omega}))^2 :\ \mathbf{v}_h|_T \in P_2 \times P_2,\ \forall T \in \mathcal{T}_h\}, \tag{4.1}$$

$$L_h^2 = \{q_h \in C^0(\overline{\Omega}) :\ q_h|_T \in P_1,\ \forall T \in \mathcal{T}_h\}, \tag{4.2}$$

respectively. The space $(H_0^1(\Omega))^2$ is then approximated by $V_{0h} = \{\mathbf{v}_h \in V_h : \mathbf{v}_h = \mathbf{0}\, on\, \Gamma\}$. This is the *Taylor-Hood* finite element approximation [13]. For the discretization of the Lagrange multipliers $\boldsymbol{\lambda}(t)$, we can approximate the functional spaces $\Lambda(t) = (H^1(B(t)))^2$ by a finite element on a grid defined on the rigid body $B(t)$. However we prefer the following alternative that is easier to implement: let $\{\mathbf{x}_i\}_{i=1}^N$ be a set of points from $\overline{B(t)}$ which cover $\overline{B(t)}$. We define

$$\Lambda_h(t) = \{\boldsymbol{\mu}_h : \boldsymbol{\mu}_h = \sum\nolimits_{i=1}^N \boldsymbol{\mu}_i \delta(\mathbf{x} - \mathbf{x}_i),\ \boldsymbol{\mu}_i \in \mathbb{R}^2,\ \forall i = 1, ..., N\}, \tag{4.3}$$

where $\delta(\cdot)$ is the Dirac measure at $\mathbf{x} = \mathbf{0}$. Then, instead of the scalar product of $(H^1(B_h(t)))^2$ we use $< \cdot, \cdot >_h$ defined by

$$< \boldsymbol{\mu}_h, \mathbf{v}_h >_h = \sum\nolimits_{i=1}^N \boldsymbol{\mu}_i \cdot \mathbf{v}_h(\mathbf{x}_i),\ \forall \boldsymbol{\mu}_h \in \Lambda_h(t),\ \mathbf{v}_h \in V_h. \tag{4.4}$$

This approach makes little sense for the continuous problem, but is meaningful for the discrete problem; it amounts to forcing the rigid body motion of $B(t)$ via a *collocation method*. A similar technique has been used to enforce Dirichlet boundary conditions by Bertrand *et al.* [1].

5. Time Discretization by Operator Splitting. After space discretization of (3.1)–(3.6) by the finite element method, we obtain an initial value problem of the form

$$\frac{d\varphi}{dt} + \sum_{i=1}^{4} A_i(\varphi, t) = f, \ \varphi(0) = \varphi_0, \tag{5.1}$$

where the operators A_i can be *multivalued*, and are associated to each of the following numerical difficulties: (i) the incompressibility condition and the related unknown pressure, (ii) an advection term, (iii) a diffusion term, (iv) the rigid body motion of the $B_h(t)$ and the related multipliers $\boldsymbol{\lambda}_h(t)$. The following fractional step method à la Marchuk-Yanenko [10] is used to solve this problem: *Given* $\varphi^0 = \varphi_0$, *for* $n \geq 0$, *compute* φ^{n+1} *from* φ^n *via*

$$\frac{\varphi^{n+i/4} - \varphi^{n+(i-1)/4}}{\Delta t} + A_i(\varphi^{n+i/4}, (n+1)\Delta t) = f_i^{n+1}, \quad i = 1, ..., 4, \tag{5.2}$$

with $\sum_{i=1}^{4} f_i^{n+1} = f^{n+1}$, and Δt a time discretization step. An application of this scheme to the finite element formulation of (3.1)–(3.6) results in the following equations: *Given* $\mathbf{u}^0 = \mathbf{u}_{0h}$, ϕ^0, ω^0, B^0, *for* $n \geq 0$, *knowing* $\mathbf{u}^n$, ϕ^n, ω^n, B^n, *compute* $\mathbf{u}^{n+1/4} \in V_{0h}$, *and* $p^{n+1/4} \in L^2_{0h}$ *via the solution of*

$$\begin{cases} \rho_f \displaystyle\int_\Omega \frac{\mathbf{u}^{n+1/4} - \mathbf{u}^n}{\Delta t} \cdot \mathbf{v} d\mathbf{x} - \int_\Omega p^{n+1/4} \boldsymbol{\nabla} \cdot \mathbf{v} d\mathbf{x} = 0, \ \forall \mathbf{v} \in V_{0h}, \\ \displaystyle\int_\Omega q \boldsymbol{\nabla} \cdot \mathbf{u}^{n+1/4} d\mathbf{x} = 0, \ \forall q \in L^2_h. \end{cases} \tag{5.3}$$

Compute $\mathbf{u}^{n+2/4} = \mathbf{u}(t^{n+1}) \in V_{0h}$, *where* $\mathbf{u}(t)$ *is the discrete solution of the following pure advection problem on* (t^n, t^{n+1})

$$\begin{cases} \displaystyle\int_\Omega \frac{\partial \mathbf{u}}{\partial t} \cdot \mathbf{v} d\mathbf{x} + \int_\Omega (\mathbf{u}^{n+1/4} \cdot \boldsymbol{\nabla}) \mathbf{u} \cdot \mathbf{v} d\mathbf{x} = 0, \ \forall \mathbf{v} \in V_{0h}, \\ \mathbf{u}(t^n) = \mathbf{u}^{n+1/4}. \end{cases} \tag{5.4}$$

Next, find $\mathbf{u}^{n+3/4} \in V_{0h}$ *by solving the diffusion problem*

$$\rho_f \int_\Omega \frac{\mathbf{u}^{n+3/4} - \mathbf{u}^{n+2/4}}{\Delta t} \cdot \mathbf{v} d\mathbf{x} + \mu_f \int_\Omega \boldsymbol{\nabla} \mathbf{u}^{n+3/4} : \boldsymbol{\nabla} \mathbf{v} d\mathbf{x} = \rho_f \int_\Omega \mathbf{g} \cdot \mathbf{v} d\mathbf{x}, \ \forall \mathbf{v} \in V_{0h}. \tag{5.5}$$

Now, predict the position and velocity of the rigid body by solving

$$\frac{d\omega}{dt} = -\frac{M\, g\, l\, sin\phi}{(M\, l^2 + I)}, \quad and \quad \frac{d\phi}{dt} = \omega, \tag{5.6}$$

on $t^n < t < t^{n+1}$, *with* $\phi(t^n) = \phi^n$, *and* $\omega(t^n) = \omega^n$. *Then set* $\phi^{n+3/4} = \phi(t^{n+1})$, *and* $\omega^{n+3/4} = \omega(t^{n+1})$. *Finally, we enforce the rigid body motion in the region* $B(t^{n+3/4})$ *by solving for* $\mathbf{u}^{n+1}$, $\boldsymbol{\lambda}^{n+1}$, *and* ω^{n+1} *the following equation*

$$\begin{cases} \rho_f \displaystyle\int_\Omega \frac{\mathbf{u}^{n+1} - \mathbf{u}^{n+\frac{3}{4}}}{\Delta t} \cdot \mathbf{v} d\mathbf{x} + (1 - \frac{\rho_f}{\rho_B})(M\, l^2 + I) \frac{\omega^{n+1} - \omega^{n+\frac{3}{4}}}{\Delta t} \theta = \\ < \boldsymbol{\lambda}^{n+1}, \mathbf{v} - \boldsymbol{\theta} \times \overrightarrow{\mathbf{Ox}}^{n+\frac{3}{4}} > \quad \forall \mathbf{v} \in V_{0h}, \ \forall \theta \in \mathbb{R}, \\ < \boldsymbol{\mu}_j, \ \mathbf{u}^{n+1} - \boldsymbol{\omega}^{n+1} \times \overrightarrow{\mathbf{Ox}}^{n+\frac{3}{4}} >= 0, \quad \forall \boldsymbol{\mu}_j \in \Lambda_h^{n+\frac{3}{4}}. \end{cases} \tag{5.7}$$

Problems (5.3) and (5.7) are finite dimensional linear saddle-point problems which are solved by an *Uzawa/conjugate gradient algorithm* [6]. The pure advection problem (5.4) is solved by the wave-like equation method discussed in Dean *et al.* [4] and [5]. Problem (5.5) is a discrete elliptic system whose iterative or direct solution is a quite classical problem. In this work all the linear systems are solved by a sparse matrix algorithm based on Markowitz' method [11]

6. Numerical Experiments and Conclusions. We consider a two-dimensional rectangular domain $\Omega = (-3, 3) \times (-1, 1)$ filled with a viscous fluid of density $\rho_f = 1$. The axis of rotation of the pendula is fixed at $\mathbf{O} = (0, 1)$, and the diameter of the circular rigid bodies is 0.25 in all cases bellow.

As a test case we consider one pendulum with a circular rigid body of density $\rho_B = 3$ released from rest at $\phi^0 = 1.4$ radians in a liquid of viscosity $\mu_f = 0.005$. We solved this problem using two meshes: an unstructured mesh (Fig. 6.1) which takes advantage that we know in advance the possible trajectory of the rigid body, and a uniform mesh with space discretization step $h = 1/64$. Figure 6.2 shows the comparison of the time history of the angle and of the angular velocity obtained with the two meshes. The agreement is satisfactory. As expected, the pendulum exhibits damped oscillations around the vertical position, and it goes to a steady position as time increases. The maximum Reynolds number obtained (based on the maximum falling velocity and diameter of the circular rigid body) was 835. Since the unstructured mesh has much less velocity degrees of freedom than the regular mesh (13823 versus 49665), we used the unstructured mesh in the subsequent calculations.

As a second example we consider two pendula. One pendulum with a circular rigid body of density $\rho_1 = 1.1$ is initially hold in the vertical position $\phi_1^0 = 0$, and the other pendulum with density $\rho_2 = 5$ is released from rest at $\phi_2^0 = 1.4$ radians in a liquid of viscosity $\mu_f = 0.005$. Figure 6.3 shows that, after a short time, the heavier cylinder collides with the lighter fixed body. After collision the two bodies move together as a single body all the time. This is more evident in in Figure 6.4 where the time history of the angle, angular velocity, and separation distance is shown. The maximum Reynolds number in this case was 1,085. We expected the two bodies to separate after they reach the maximum negative angle since the heavier rigid body is below to the lighter one at that position, and the action of gravity is stronger on the heavier body. However they never separate after collision. The only forces in our model problem that can prevent separation after collision are the viscous forces which in this case seem to dominate. To corroborate this strong dependence from viscous effects, we reduced μ_f from 0.005 to 0.001 and repeated the numerical calculation. Figure 6.5 shows that this time, after the two bodies collide, they stick together until they reach the maximum negative angle (where the angular velocity is close to zero), and then separate when they start to move in the counterclockwise direction by the action of gravity. This is clearly shown in Figure 6.6 where we plot the time history of angle, angular velocity, and separation distance. The maximum Reynolds number this time was 5,800. It is evident that a more detailed study of this and related phenomena is needed in order to better understand the mechanics of particle collision in viscous liquids and to generate models that simulate more accurately solid-liquid particulate flows which are very important in applications.

REFERENCES

[1] F. Bertand, P. A. Tanguy, and F. Thibault. A three-dimensional fictitious domain method for incompressible fluid flow problems. *Int. J. Num. Meth. Fluids*, 1997.

[2] R. E. Cox and H. Brenner. The slow motion of a sphere through a viscous fluid towards a plane surface–II. Small gap widths including inertial effects. *Chem. Engng. Sci.*, 22:1753, 1967.

[3] R. A. Davis, J. M. Serayssol, and E. J. Hinch. The elastohydrodynamic collision of two spheres. *J. Fluid Mech.*, 163:479–497, 1986.

[4] E. J. Dean and R. Glowinski. A wave equation approach to the numerical solution of the Navier-Stokes equations for incompressible viscous flow. *C.R. Acad. Sc. Paris*, 325(Serie 1):783–791, 1997.

[5] E. J. Dean, R. Glowinski, and T. W. Pan. A wave equation approach to the numerical simulation of incompressible viscous flows modeled by the Navier-Stokes equations. In J. A. D. Santo, editor, *Mathematical and Numerical Aspects of Wave Propagation*, pages 65–74, Philadelphia, PA, 1998. SIAM.

[6] R. Glowinski and P. Le Tallec. Augmented Lagrangian and operator splitting methods in nonlinear mechanics. In T. F. Chan, R. Glowinski, J. Périaux, and O. B. Widlund, editors, *Proc. 2nd International Symposium on Domain Decomposition Methods*, Philadelphia, 1989. SIAM.

[7] R. Glowinski, T.-W. Pan, T. I. Hesla, D. D. Joseph, and J. Periaux. A fictitious domain approach to the direct numerical simulation of incompressible viscous flow past moving rigid bodies: Application to particulate flow. *J. Comput. Phys.*, 169:363–426, 2001.

[8] H. H. Hu, D. D. Joseph, and M. Crochet. Direct simulation of fluid particle motions. *Theoret. Comput. Fluid Dynamics*, 3:285–306, 1992.

[9] G. Joseph, R. Zenit, M. Hunt, and A. Rosenwinkel. Particle-wall collision in a viscous fluid. *J. Fluid Mech.*, 433:329–346, 2001.

[10] G. I. Marchuk. *Handbook of Numerical Analysis, Splitting and alternating direction methods*, volume I. Elsevier Science Publishers B.V., North-Holland, Amsterdam, 1990.

[11] S. Pissanetzky. *Sparse Matrix Technology.* Academic Press, 1984.

[12] Y. Roux, E. Rivoalen, and B. Marichal. Vibrations induites d'un pendule hydrodynamique. *C. R. Acad. Sci. Paris*, 328(Série II b):479–497, 2000.

[13] C. Taylor and P. Hood. A numerical solution of the Navier-Stokes equations using the finite element method. *Comput. & Fluids*, 1:73–100, 1973.

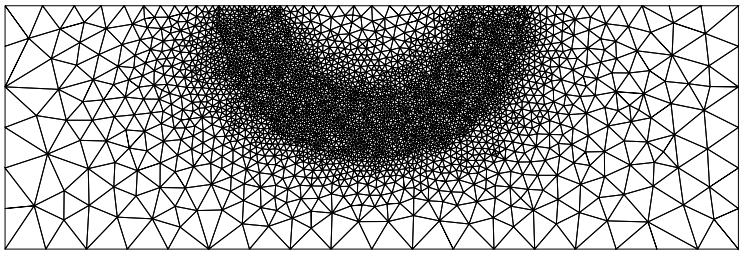

Figure 6.1: The unstructured mesh

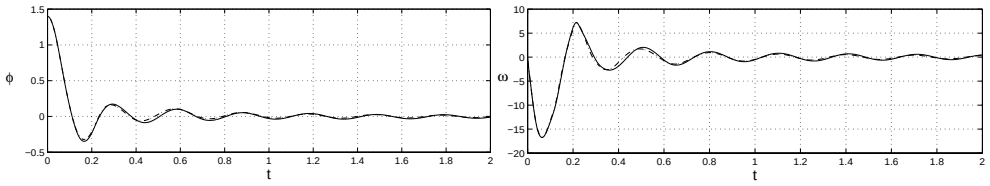

Figure 6.2: Comparison of the time history of the angle (left) and of the angular velocity (rigth) obtained with the unstructured mesh (dashed line) and the regular mesh (continuous line) for one pendulum

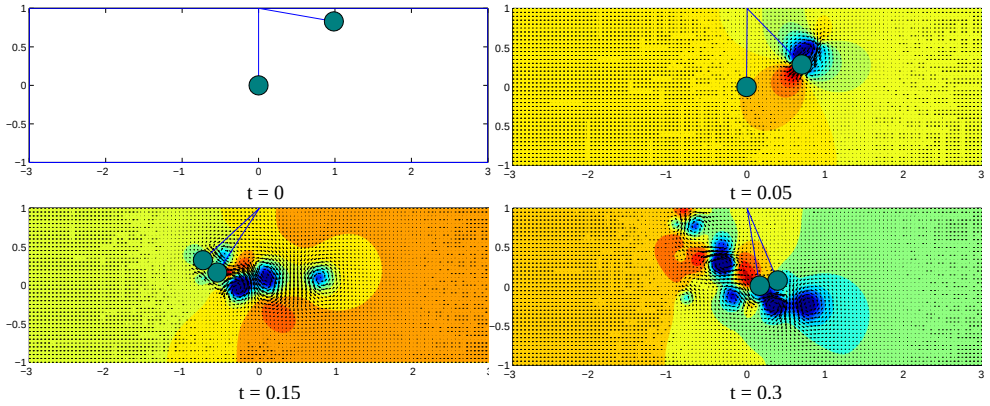

Figure 6.3: Velocity vector field and pressure at different times for the two pendula with $\mu_f = 0.005$, $\rho_1 = 1.1$, and $\rho_2 = 5$.

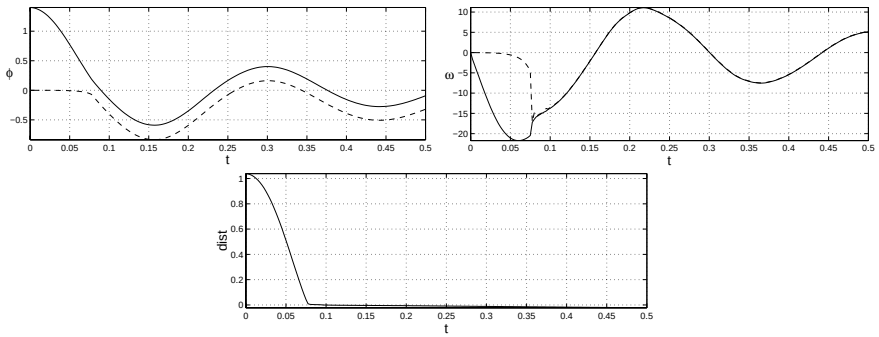

Figure 6.4: Time history of the angle (top left), angular velocity (top right), and separation distance (bottom) of the two pendula with $\mu_f = 0.005$, $\rho_1 = 1.1$, and $\rho_2 = 5$.

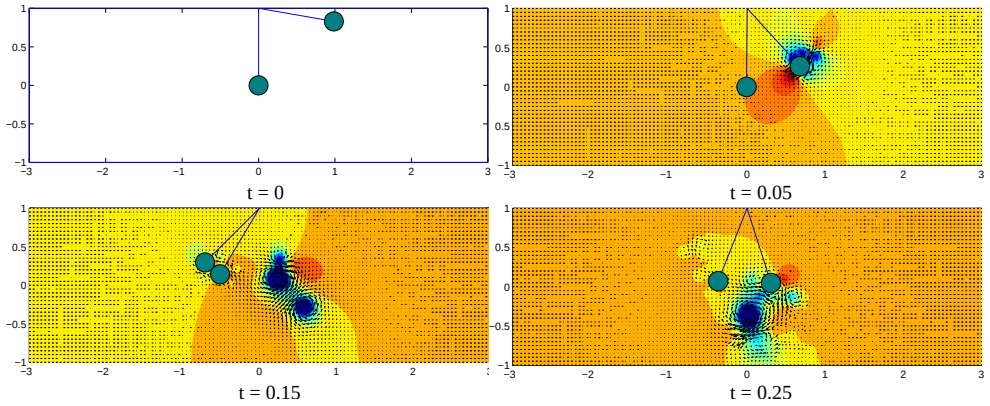

Figure 6.5: Velocity vector field and pressure at different times for the two pendula with $\mu_f = 0.001$, $\rho_1 = 1.1$, and $\rho_2 = 5$.

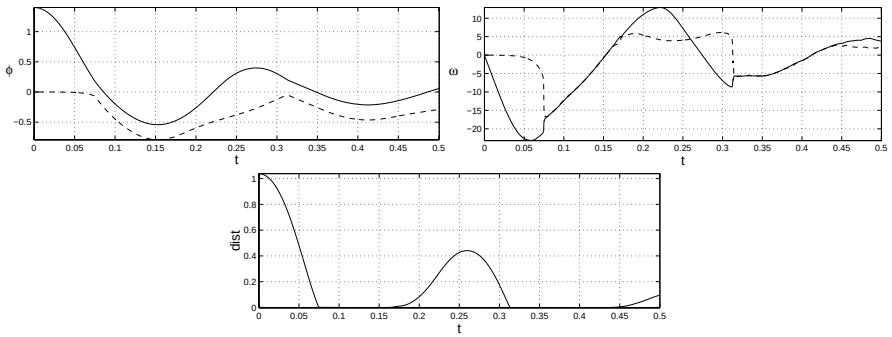

Figure 6.6: Time history of the angle (top left), angular velocity (top right), and separation distance (bottom) of the two pendula with $\mu_f = 0.001$, $\rho_1 = 1.1$, and $\rho_2 = 5$.